

# Emission characteristics and dynamics of neutral species in a laser-produced tin plasma

M V Mathew, S S Harilal and M S Tillack

Center for Energy Research, University of California San Diego, 9500 Gilman Drive, La Jolla, CA 92093-0438, USA

Received 21 August 2006, in final form 20 October 2006

Published 5 January 2007

Online at [stacks.iop.org/JPhysD/40/447](http://stacks.iop.org/JPhysD/40/447)

## Abstract

We investigated the emission features of tin neutrals in a laser-ablated tin plasma using time and space resolved optical emission spectroscopy. The tin plume was generated by focusing 1064 nm, 10 ns pulses from a Nd:YAG laser on a tin slab target placed in a vacuum chamber. We examined the properties of the tin neutrals at various spatial locations from the target surface and at different laser irradiance levels. The neutral tin particles were found to be moving with a velocity close to the expansion velocity of singly charged ions at shorter distances from the target surface while their velocity was considerably reduced at distances  $>5$  mm. Spatially and temporally resolved emission studies also showed a double peak structure in the temporal profiles of excited neutral tin at shorter distances from the target surface.

(Some figures in this article are in colour only in the electronic version)

## 1. Introduction

There has been a growing interest in the field of laser-produced plasma (LPP) for some time now because of its ever-growing applications in basic and applied fields of research. Much effort has been spent on the basic understanding of LPP [1–3]. Applications of LPP ranges from pulsed laser thin film deposition [4], inertial confinement fusion [5], nanoparticle and cluster production [6], laser-induced breakdown spectroscopy [7, 8], laboratory simulation of astrophysical environment [9] and extreme-ultraviolet (EUV) lithography sources [10].

LPP from tin is considered to be a strong candidate for an EUV lithography source [10–12]. One of the most important problems confronted with a laser-induced tin plasma source is the debris from the tin plume. The debris from LPP includes energetic ions, neutrals, particulates and molten droplets [13]. Several studies have been carried out for characterizing the energetic ions from a tin plasma and various methods employed for controlling the energetic ions, including magnetic and electric fields, double pulse, ambient gas, etc [13–15]. But little effort has been spent on understanding the evolution of the fast neutrals from the tin plasma and in an EUV source it could

also act as a potential debris. In LPP, the expansion velocity of the various species is closely related to their charge states as well as the mass of the species. The species with higher charge states move with high expansion velocities compared to their counterparts with lower charge states [16], while neutrals and molecular species propagate with lower velocities [17, 18]. But neutrals can also possess high expansion velocities similar to singly ionic species if they are produced during flight from the target by recombination.

Typical diagnostic tools employed for understanding the evolution of neutrals in a plume are laser-induced fluorescence (LIF) [19] and optical time of flight-emission spectroscopy (OTOF-ES) [20]. In LIF, a probe laser is tuned in resonance with a neutral species excited level and the fluorescence signals are collected. The main advantage of the LIF method is that it provides an estimate of neutral number density [21] and it is also possible to investigate the dynamics of nonemissive neutral particles [19]. Optical emission spectroscopy (OES) is one of the simplest, non-intrusive ways to investigate early plasma dynamics since it uses intrinsic light emission from the LPP and does not require external excitation. Spectral details can also be useful for estimating the plasma ionization balance, rate processes, densities, and temperatures [22–24]. Even

though OTOF studies will not provide the number density of the excited neutral species, these studies are extremely useful for understanding how the neutral species evolve and provide the velocity distribution of excited neutral species at various locations in a plume.

In this paper, we report the evolution and dynamics of neutrals in a laser created Sn plasma employing OTOF-ES. We have studied the variation in the intensity and velocity of excited neutrals as a function of distance from the target surface and laser irradiance. Since the generation of most of the neutral particles in a plume is mainly due to recombination, we also carried out similar studies on singly ionized tin species. This will provide much physical insight into the evolution dynamics of neutrals in a laser-induced tin plasma as it expands into vacuum.

## 2. Experimental set-up

We have performed time of flight studies on various species in the plume using space resolved OES. The 1064 nm, 10 ns (FWHM) pulses from a Q-switched Nd:YAG laser operated at 10 Hz was used to create a tin plasma in a stainless steel vacuum chamber. The vacuum chamber was evacuated using a cryogenic pump and a base pressure of  $\sim 10^{-6}$  Torr was maintained. A 2 mm thick 99.9% pure tin target in the form of a disc was rotated and translated to avoid errors due to local heating and drilling. The laser beam was focused onto the target surface at normal incidence using an  $f/12$  antireflection-coated plano-convex lens. The spot radius at the target surface was  $400 \mu\text{m}$ . Laser beam energy was monitored using a thermal surface absorbing energy meter (Ophir, Model 30A).

The light emitted from the luminous plasma was transmitted through a quartz window mounted orthogonally to the direction of plume expansion. An optical system consisting of a collimating and focussing lens was used to image the plasma plume onto the entrance slit of a 0.5 m Czerny–Turner spectrograph (Acton Pro, Spectra-Pro 500i) so as to have one-to-one correspondence with the sampled area of the plume and its image. The spectrograph was equipped with three gratings: 150, 600 and  $2400 \text{ g mm}^{-1}$ . For the present work we used the grating with  $600 \text{ g mm}^{-1}$ . One of the exit ports of the spectrograph was coupled to an intensified CCD (ICCD) camera that was operated with vertical binning of the charge coupled device array to obtain spectral intensities versus wavelength. The other exit port of the monochromator was coupled to a photomultiplier tube (PMT). A diverter mirror was used for switching from PMT to ICCD or vice versa. The spectrograph and detectors were sensitive to a spectral window of 250–750 nm. For recording the temporal profiles of a particular species in the plume, the specific lines were selected by tuning the grating and imaging onto the slit of the PMT (rise time 2 ns). The output of the PMT was directly coupled to a Tektronix 500 MHz digital phosphor oscilloscope (Model TDS 5054B). This set-up provides delay as well as decay of emission of a constituent species within the plasma, which are very important parameters related to the evolution of laser-ablated materials in a direction normal to the target surface.

## 3. Results and discussions

The LPPs are highly transient in nature. The characteristic parameters of a plume created by a laser strongly depend on several factors including laser wavelength, angle of incidence of laser, spot size and irradiance at the target surface, background pressure etc. The various species in the plume travel with very high velocities and expand rapidly into the vacuum or ambient. The visible spectral details of the tin plume showed at early times that most of the emission from the tin plume was contributed by singly charged ions. At later times excited neutral species were also observed along with ionic species. Recently temperature and density measurements of a laser-generated tin plume were carried out using OES [25]. The electron density ( $n_e$ ) was measured by the Stark broadening method, and the electron temperature ( $T_e$ ) of the tin plasma was estimated by the Boltzmann plot method employing line intensities of singly ionized tin, the details of which are given in an earlier paper [25]. At earlier times, especially below 60 ns, the intense continuum radiation is dominant, making it difficult to extract line intensities and profiles. The line-to-continuum ratio increases as time evolves. The estimated temperature and density at 1 mm from the target surface at the early time (around 70 ns after the evolution of the plasma) is 3.2 eV and  $7.7 \times 10^{17} \text{ cm}^{-3}$ , respectively. Temporal and spatial behaviours of electron temperature and density in the laser-generated tin plasma have been analysed. Time evolutions of density and temperature are found to decay adiabatically at early times. The spatial variation of density shows approximately  $1/z$  dependence, which is consistent with an adiabatic expansion. Spatial studies of temperature showed its values near the target were more or less constant, but increased significantly for distances greater than 7 mm. A deviation from the assumption of LTE for temperature estimation is attributed for the rise in temperature at larger distances [25]. Recently Cummings *et al* [12] reported modelling results of spatio-temporal evolution of temperature and density of Sn plasma during the laser pulse and showed a temperature of 30 eV and a density of  $\sim 10^{20} \text{ cm}^{-3}$  very close to the target surface with a laser irradiance of  $2 \times 10^{11} \text{ W cm}^{-2}$ .

Typical time integrated tin spectra recorded at two different distances from the target surface are given in figure 1. The recorded spectra showed several neutral Sn lines and among them the strongest lines were Sn at 317.5 nm ( $5p^2\ ^3P-6s\ ^3P$ ) and 326.2 nm ( $5p^2\ ^1D-6s\ ^1P^0$ ). For studying time evolution of excited neutral species in a tin plume, we selected neutral Sn emission at 317.5 nm and the TOF emission profiles were recorded for distances up to 26 mm. Typical TOF profiles measured at different spatial points in the plume at a laser irradiance of  $2 \text{ GW cm}^{-2}$  are shown in figure 2. The sharp spike observed at earlier time is the prompt signal that is used as a time marker. The temporal emission features are affected by the presence of strong continuum at short distances ( $\leq 1$  mm) and at early time. But at distances greater than 1 mm, the continuum emission is considerably reduced and the interference of continuum on the TOF profiles is negligible. As figure 2 shows, the TOF profile of excited neutral tin clearly shows a double peak structure and this twin peak behaviour is evident only at a certain distance from the target surface. The faster kinetic energy peak (hereafter peak 1) of the twin

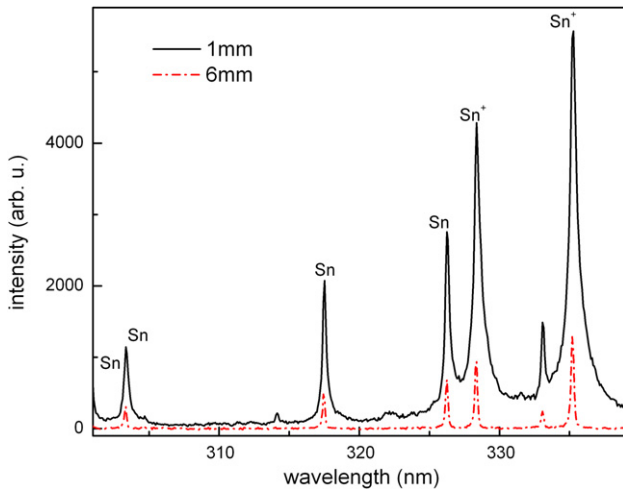


**Figure 1.** Time integrated emission spectra recorded from Sn plasma plume at two different distances from the target surface (laser irradiance used was  $2 \text{ GW cm}^{-2}$ ).

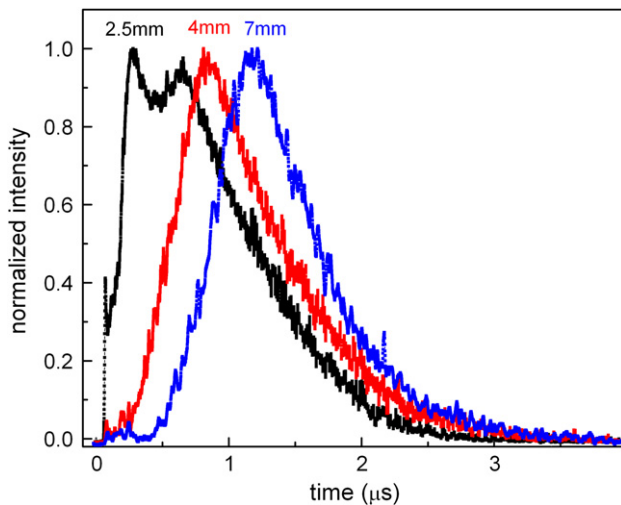


**Figure 2.** The temporal profiles of excited neutral Sn species at  $317.5 \text{ nm}$  ( $5p^2\ ^3P-6s\ ^3P$ ) recorded at different distances from the target surface at a laser irradiance of  $2 \text{ GW cm}^{-2}$ .

peak structure exists for distances very close to the target and is almost non-existent after about  $4 \text{ mm}$  from the target. The slower kinetic peak (hereafter peak 2) exists at all distances, except at very close distances from the target surface. It seems that the peak 2 of Sn might exist even at distances smaller than  $2 \text{ mm}$ , since the intensity of peak 1 is very high at shorter distances, it may immerse the slower kinetic energy species in their decay part.

The observation of multiple peak structures in the TOF profiles were previously reported by several groups in laser-generated plasmas [26–30]. Recently, a multiple peak temporal structure was observed for neutral and singly ionized aluminium species. As the plume expands into an ambient, gas phase collisions transform the initial temporal distribution into a very different final distribution. Such deformations in the TOF profiles occurred at larger distances from the target surface ( $>5 \text{ mm}$ ). Amoruso *et al* [27] observed a double-peak structure in the kinetic energy distribution of ions species during TOF mass spectroscopic studies of laser-ablated copper

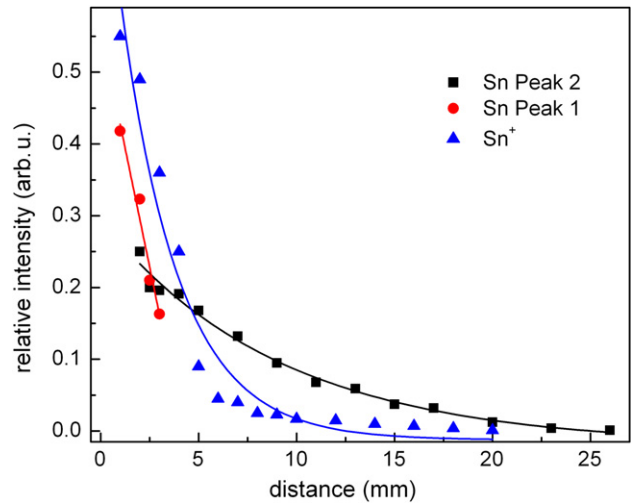


**Figure 3.** Variation in the maximum emission intensity of faster and slower peaks of neutral Sn and peak of  $\text{Sn}^+$  as a function of distance from the target. The points represent the data and the solid lines give the best fit (laser irradiance used was  $2 \text{ GW cm}^{-2}$ ).

plasma and they ascribed the origin of low kinetic peak due to the thermo-ionic component. Most of the reported occurrence of double-peak distribution in TOF profiles happened when the plume interacts with a background gas. In the presence of a moderate ambient pressure ( $0.05\text{--}500 \text{ mTorr}$ ), the deformation in the temporal profiles of various species can happen because a group of species interpenetrate into the background gas without losing much kinetic energy, while a collection of species lose their energy during collision with background gas species. Fast frame photography of the plume propagation revealed that the background gas has a negligible effect when the plume propagated into an ambient with a pressure of less than  $10^{-2} \text{ Torr}$  [18, 31]. Hence in the present studies, gas dynamic effects are negligible as the plume expands freely into vacuum.

In a LPP, the production of excited neutral particles is mainly due to three-body recombination. So for better understanding of the generation and evolution of neutral species, we also carried out space and time resolved studies of singly ionized Sn species. For TOF studies  $\text{Sn}^+$  at  $335.2 \text{ nm}$  ( $4f^2\ ^1F-5p^2\ ^2D$ ) is selected (see figure 1). The recorded TOF profiles of  $\text{Sn}^+$  showed only single peak distribution at all spatial locations studied.

The intensity of the peak emission estimated from the temporal profiles for Sn and  $\text{Sn}^+$  as a function of the distance from the target is given in figure 3. The intensity of  $\text{Sn}^+$  and peak 1 of Sn decreases exponentially from the target surface. This is due to cooling of the plume by recombination. The prominent recombination in a LPP is three-body recombination [32]. In three-body recombination an electron is initially captured by an upper excited level. The electron then cascades down to the ground state either by radiative transitions or by transferring energy to free electrons through collisions. Figure 3 also suggests that the intensity of the peak 1 of Sn should be non-zero at distances  $\geq 4 \text{ mm}$ . It indicates that the peak 1 will be present at higher distances, but it is not observable in the TOF profiles as the intensity of peak 2 is much higher at these distances (the rising part of the peak 2 can immerse the peak 1).

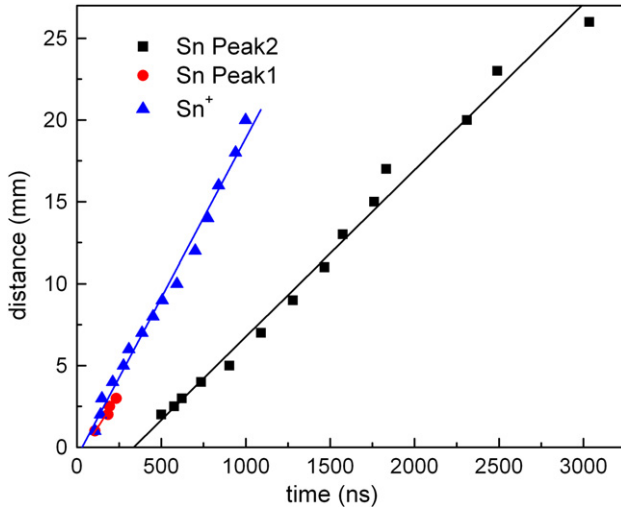


**Figure 4.** Variation in the time delay of peak 1 and peak 2 of excited neutral Sn as well as peak Sn<sup>+</sup> for different distances from the target surface. The solid lines represent the linear fit (laser irradiance used was 2 GW cm<sup>-2</sup>).

Variation in time delay of various Sn species with distance from the target is given in figure 4. It can be easily noticed that the peak 2 of excited neutral Sn is much delayed compared with the peak 1 of excited neutral Sn and Sn<sup>+</sup>. The expansion velocities of the different species are estimated from the position–time plots. The peak 1 of neutral Sn species moves with a velocity of  $(1.1 \pm 0.2) \times 10^6$  cm s<sup>-1</sup> while the expansion velocity of the peak 2 is found to increase steadily with distance and attain a constant value ( $\sim 9 \pm 1$ )  $\times 10^5$  cm s<sup>-1</sup> at distances  $\geq 12$  mm. The expansion velocity of tin ions is found to be  $(1.8 \pm 0.2) \times 10^6$  cm s<sup>-1</sup>, which corresponds to a kinetic energy of 200 eV. The initial increase in the velocity of Sn and Sn<sup>+</sup> species with distance from the target is due to the initial acceleration of the species from zero velocity, which attains its maximum and remains almost constant thereafter. It could be seen that the Sn<sup>+</sup> moves at a higher velocity compared with neutral Sn. This is due to the coulomb fields generated by negatively charged electrons escaping from the plume. Cummings *et al* [12] modelling results showed that Sn ions possess roughly one order higher kinetic energy at a distance of 2 mm from the target surface compared with the present experimental results. But they have not provided the kinetic energy possessed by low charged ions (e.g. Sn<sup>+</sup>, Sn<sup>2+</sup>, etc) and neutrals.

In order to get more details about the origin of faster Sn species, we also examined the influence of laser irradiance on the TOF profiles of Sn and Sn<sup>+</sup> species at a distance of 2.5 mm from the target surface. The selection of the 2.5 mm spatial segment from the target surface is based on the fact that at these distances we observed a peculiar dual-peak structure for neutral tin species. Both the kinetic peaks of neutral tin species are prominent at low irradiance levels. At higher laser irradiance levels ( $>4$  GW cm<sup>-2</sup>) the intensity of the peak 1 of Sn becomes very prominent than the delayed peak immersed in the decay part of the faster peak. Figure 5 shows the variation in line intensities obtained from TOF profiles as a function of laser irradiance measured at a distance of 2.5 mm from the target. The intensity of Sn<sup>+</sup> is found to be

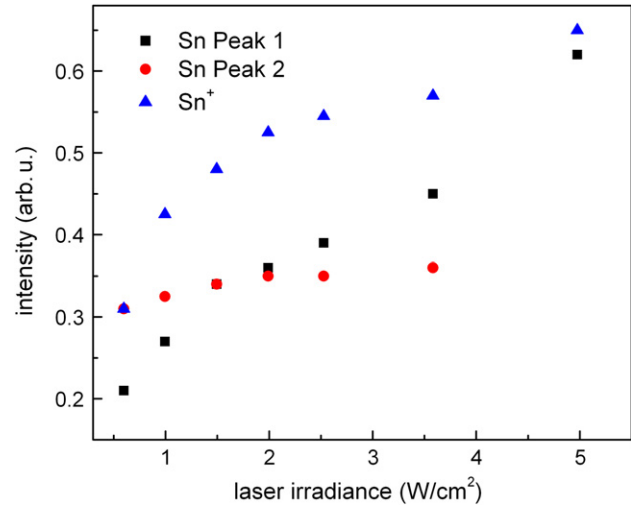


**Figure 5.** Variation in various line intensities as a function of laser irradiance measured at a distance of 2.5 mm from the target.

higher than neutrals even at the lowest laser irradiance used in the present studies. The first ionisation potential of Sn is 7.34 eV and the reported threshold irradiance [16] for the production of Sn<sup>+</sup> under similar experimental conditions is 0.16 GW cm<sup>-2</sup>. In the present studies the lowest irradiance used is 0.5 GW cm<sup>-2</sup>, which is much higher than the reported threshold. As laser irradiance increases an enhancement in the line intensities is observed for all species caused by rise in the plasma temperature. The peak 1 of neutral Sn and Sn<sup>+</sup> show a rapid increase in intensity with laser irradiance. The intensity of the peak 2 of Sn shows a much lesser increase with laser irradiance and almost saturates at higher laser irradiance levels.

It should be noted that a change in laser irradiance can significantly influence the amount of ablated mass and hence the crater volume. Depending on the laser irradiance and target material, mass removal can occur through desorption, thermal evaporation, exfoliation, phase explosion and other mechanisms. The threshold for occurring the above processes strongly depended on the laser wavelength and the laser spot size at the target surface. For example, Yoo *et al* [33] reported that the laser irradiance threshold for phase explosion is roughly one order higher with 532 nm than with 266 nm. They have not observed any rapid change in crater volume with 1064 nm in the studied laser irradiance range ( $1\text{--}10^3$  GW cm<sup>-2</sup>) and explained it as being due to stronger plasma shielding and deeper optical penetration depth with the increasing wavelength.

Figure 6 shows the variation in the time delay of various peaks with laser irradiance observed at a distance of 2.5 mm from the target. The time delay of the peak 2 of Sn shows a decrease with laser irradiance, whereas the time delay of the peak 1 of Sn and the peak of Sn<sup>+</sup> decrease initially and then increase with laser irradiance, which contradicts the standard observation of increased kinetic energy at higher laser intensities. Pappas *et al* [34] also observed similar behaviour for C<sub>2</sub> species and explained it as preferential dissociation by electron impact. With increasing laser energy, higher charged species (Sn<sup>2+</sup>, Sn<sup>3+</sup>, etc) will be present in the plasma, especially close to the target surface. The reported

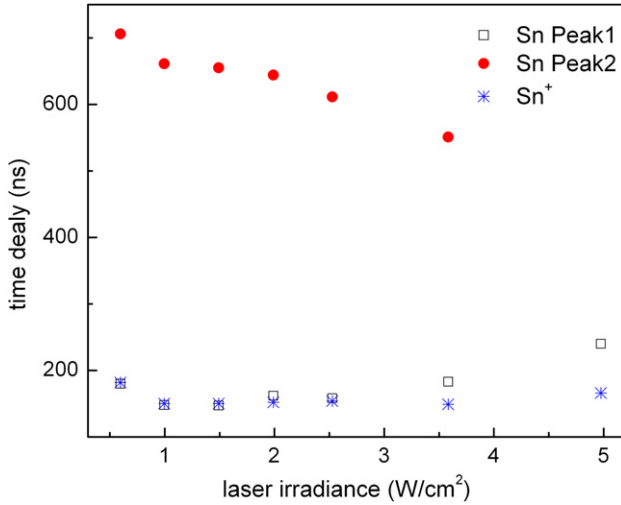


**Figure 6.** The variation in the time delay of various peaks with laser irradiance observed at a distance of 2.5 mm from the target.

ionization threshold for  $\text{Sn}^{2+}$  and  $\text{Sn}^{3+}$  are  $0.24 \text{ GW cm}^{-2}$  and  $1.3 \text{ GW cm}^{-2}$ , respectively [16]. The emission from these highly charged tin ions are concentrated in the wavelength region lower than 200 nm [35] and the spectral diagnosing system used in the present experiment is not capable of detecting it. The increase in ionization with varying laser irradiance also seems to suggest strong interaction of the laser pulse with the dense plasma formed near the target within the pulse duration. In another words, after the creation of the plasma, the target is screened off from the remaining part of the laser beam because of laser absorption by the plasma due to inverse bremsstrahlung [36]. The laser plasma interaction eventually heats up the plasma and more highly charged ions are produced. Hence the fast moving  $\text{Sn}^+$  and Sn species can be depleted because of ionization, which will eventually affect the TOF profiles.

TOF data from a LPP can often be represented by a shifted Maxwell–Boltzmann (SMB) distribution with a centre of mass shifted streaming velocity given by

$$f(v) = A \left( \frac{m}{2\pi k} \right)^{3/2} v^3 e^{-m(v-v_0)^2/2kT} dv, \quad (1)$$

where  $A$  is the normalization parameter,  $v$  and  $v_0$  are the velocities of the species and centre of mass velocity,  $T$  is the translational temperature,  $k$  is the Boltzmann constant and  $m$  is the mass of the species. The SMB distribution assumes that the speed distribution has equilibrated after propagating a short distance from the target surface, and that the signal is a direct measure of the concentration of the indicated species. Figure 7 gives the TOF profile recorded for Sn species at 2.5 mm from the target surface in vacuum along with SMB fits for both the kinetic peaks. As the figure shows, the SMB distribution fits reasonably well with both the peaks with the fitting parameters that are given in the figure caption.

With an indirect diagnostic tool such as OES used in the present experiments, it is very difficult to elucidate the exact mechanism for the formation of double peak in the temporal profile of neutral species. Nevertheless, by considering the spatial evolution of these species along with its laser irradiance

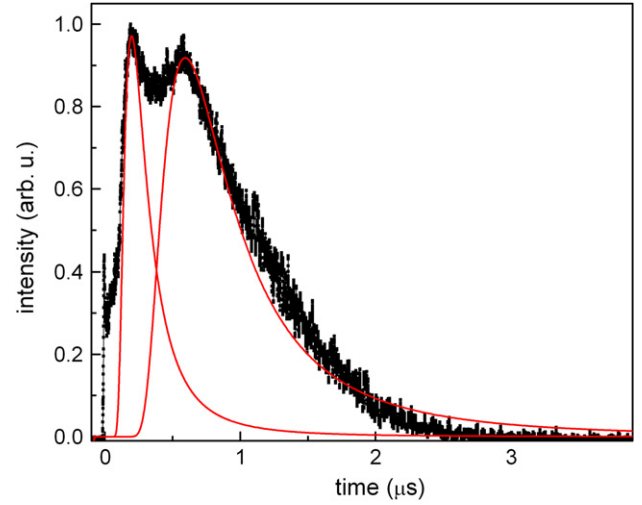


**Figure 7.** Intensity variation of spectral emission with time for Sn species ( $317.5 \text{ nm}$ ,  $5p6s^3P_1^0-5p^23P_2$ ) recorded at 2.5 mm from the target surface. The solid lines represent SMB fits for both peaks. (The fitting parameters are for peak 1,  $v_0 = 100 \text{ m s}^{-1}$ ,  $kT = 100 \text{ eV}$  and for peak 2,  $v_0 = 100 \text{ m s}^{-1}$  and  $kT = 12 \text{ eV}$ .)

dependence we made some conclusions, even though they are speculative. Since the present experiments were done in vacuum, we can easily rule out the gas dynamic effects. So the existence of dual peak in the TOF profiles of Sn can be related to the different origins of the same species in the plume. It is worth noting that the dynamics of peak 1 of Sn, which is observed only at shorter distances, followed approximately the dynamics of the  $\text{Sn}^+$  species (see figures 2–5). It indicates that the origin of the fast component of neutral tin may be related to  $\text{Sn}^+$ . Species like neutral Sn is generated directly from the target surface during ablation or generated away from the target due to recombination while  $\text{Sn}^+$  is produced mainly just outside the target due to electron impact. In the vicinity of the target surface, the temperature is so high that ionization of Sn by electron collision is highly probable. In a LPP ions move with much faster velocities than the neutrals because of the Coulomb fields exerted by the fast moving electrons. These fast moving ions can recombine with the electrons at short distances from the target surface that lead to the formation of neutrals with higher kinetic energies. The reported values of temperature and density at later stages ( $>100 \text{ ns}$ ) of tin plasma evolution was of the order of  $1 \text{ eV}$  and  $10^{16}-10^{17} \text{ cm}^{-3}$ , showing the plasma is in the recombinational regime [25]. However, the recombination will rapidly decrease as the plasma density decreases during the hydrodynamic expansion. The electron density drops very rapidly with space (proportional to  $1/Z^3$ ) as the plume expands into vacuum and hence the probability of recombination is also diminished at larger distances from the target as the 3-body recombination rate scales as  $n_e^2 T_e^{-9/2}$ .

#### 4. Summary

The evolution dynamics of neutral species in laser-produced Sn plasma have been studied using TOF emission spectroscopy. Our studies indicate that the neutral Sn species possess high expansion velocities similar to singly ionized Sn near the target surface, but at larger distances they move with half the velocity

of Sn<sup>+</sup>. The temporal profiles of excited neutral and singly ionized tin species showed distinct features at various distances from the target surface. At short distances (<5 mm), a twin peak structure is observed for neutral tin species while singly ionized Sn showed only single peak temporal profiles at all distances studied. Since all the measurements were done in vacuum, the gas dynamics effects play no role in the occurrence of double peak structure. Although no single piece of data provides decisive proof, all the evidence suggests that the origin of multiple peaks in the temporal profiles of neutral Sn at closer distances to the target surface is due to different origins for the same species occurring in the plasma. Neutral species can be generated during the ablation process as well as recombination of Sn ions. Because of the Coulomb fields exerted by the fast moving electrons, Sn<sup>+</sup> ions have higher kinetic energies than neutrals. As plasma cools, these Sn ions recombine with electrons during the flight resulting in a higher energetic component in the temporal profiles of neutral tin. The Sn neutrals created during ablation and/or generated in the vicinity of the target surface may not have any acceleration from the electrons and propagate slowly.

## References

- [1] Radziemski L J and Cremers D A 1989 *Laser-induced Plasmas and Applications* (New York: Dekker)
- [2] Chen Z Y, Bleiner D and Bogaerts A 2006 *J. Appl. Phys.* **99** 063304
- [3] Butz-Jorgensen C V, Mond M M, Doggett B and Lunney J G 2005 *J. Phys. D: Appl. Phys.* **38** 1892–8  
Butz-Jorgensen C V, Mond M M, Doggett B and Lunney J G 2006 *J. Phys. D: Appl. Phys.* **39** 4739 (corrigendum)
- [4] Chrisey D B and Hubler G K 1994 *Pulsed Laser Deposition of Thin Films* (New York: Wiley)
- [5] Epstein R 1997 *J. Appl. Phys.* **82** 2123–39
- [6] Tillack M S, Blair D W and Harilal S S 2004 *Nanotechnology* **15** 390–403
- [7] Lee W B, Wu J Y, Lee Y I and Sneddon J 2004 *Appl. Spectrosc. Rev.* **39** 27–97
- [8] Tognoni E, Palleschi V, Corsi M and Cristoforetti G 2002 *Spectrochim. Acta B* **57** 1115–30
- [9] Remington B A, Arnett D, Drake R P and Takabe H 1999 *Science* **284** 1488–93
- [10] Stamm U 2004 *J. Phys. D: Appl. Phys.* **37** 3244–53
- [11] Harilal S S, O'Shay B, Tillack M S, Tao Y, Paguio R, Nikroo A and Back C A 2006 *J. Phys. D: Appl. Phys.* **39** 484–7
- [12] Cummings A, O'Sullivan G, Dunne P, Sokell E, Murphy N, White J, Hayden P, Sheridan P, Lysaght M and O'Reilly F 2006 *J. Phys. D: Appl. Phys.* **39** 73–93
- [13] Takenoshita K, Kay C S, Teerawattanasook S and Richardson M 2005 *Proc. SPIE* **5751** 5751–64
- [14] Harilal S S, Tillack M S, O'Shay B, Tao Y, Paguio R and Nikroo A 2006 *Opt. Lett.* **31** 1549–51
- [15] Harilal S S, O'Shay B and Tillack M S 2005 *J. Appl. Phys.* **98** 036102
- [16] Torrisi L and Margarone D 2006 *Plasma Sources Sci. Technol.* **15** 635–41
- [17] Harilal S S, Issac R C, Bindhu C V, Nampoory V P N and Vallabhan C P G 1997 *J. Appl. Phys.* **81** 3637–43
- [18] Harilal S S, Bindhu C V, Tillack M S, Najmabadi F and Gaeris A C 2003 *J. Appl. Phys.* **93** 2380–8
- [19] Kumuduni W K A, Nakayama Y, Nakata Y, Okada T and Maeda M 1993 *J. Appl. Phys.* **74** 7510–6
- [20] Harilal S S 2001 *Appl. Surf. Sci.* **172** 103–9
- [21] Williamson T P, Martin G W, El-Astal A H, Al-Khateeb A, Weaver I, Riley D, Lamb M J, Morrow T and Lewis C L S 1999 *Appl. Phys. A* **69** S859–63
- [22] Doria D, Kavanagh K D, Costello J T and Luna H 2006 *Meas. Sci. Technol.* **17** 670–4
- [23] Siegel J, Epurescu G, Perea A, Gordillo-Vazquez F J, Gonzalo J and Afonso C N 2004 *Opt. Lett.* **29** 2228–30
- [24] Perez-Tijerina E, Bohigas J and Machorro R 2001 *J. Appl. Phys.* **90** 3192–9
- [25] Harilal S S, O'Shay B, Tillack M S and Mathew M V 2005 *J. Appl. Phys.* **98** 013306
- [26] Laube S J P and Voevodin A A 1998 *Surf. Coat. Technol.* **105** 125
- [27] Amoruso S, Berardi V, Bruzzese R, Spinelli N and Wang X 1998 *Appl. Surf. Sci.* **129** 953–8
- [28] Park S M and Moon J Y 1998 *J. Chem. Phys.* **109** 8124–9
- [29] An C W, Lu Y F, Goh Y W and Tan E 2000 *Appl. Surf. Sci.* **154** 269–75
- [30] Harilal S S, Bindhu C V, Tillack M S, Najmabadi F and Gaeris A C 2002 *J. Phys. D: Appl. Phys.* **35** 2935–8
- [31] Amoruso S, Sambri A and Wang X 2006 *J. Appl. Phys.* **100** 013302
- [32] Griem H R 1997 *Principles of Plasma Spectroscopy* (Cambridge, UK: Cambridge University Press)
- [33] Yoo J H, Borisov O V, Mao X and Russo R E 2001 *Anal. Chem.* **73** 2288–93
- [34] Pappas D L, Saenger K L, Cuomo J J and Dreyfus R W 1992 *J. Appl. Phys.* **72** 3966–70
- [35] <http://physics.nist.gov>
- [36] Bindhu C V, Harilal S S, Tillack M S, Najmabadi F and Gaeris A C 2003 *J. Appl. Phys.* **94** 7402–7